LETTERS
PUBLISHED ONLINE: 12 OCTOBER 2015 | DOI: 10.1038/NGEO2558
nature geoscience

Abrupt changes in the southern extent of North Atlantic Deep Water during Dansgaard–Oeschger events

Julia Gottschalk[1]*, Luke C. Skinner[1], Sambuddha Misra[1], Claire Waelbroeck[2], Laurie Menviel[3,4] and Axel Timmermann[5]

The glacial climate system transitioned rapidly between cold (stadial) and warm (interstadial) conditions in the Northern Hemisphere[1]. This variability, referred to as Dansgaard–Oeschger variability[2], is widely believed to arise from perturbations of the Atlantic Meridional Overturning Circulation[3–5]. Evidence for such changes during the longer Heinrich stadials has been identified, but direct evidence for overturning circulation changes during Dansgaard–Oeschger events has proven elusive[6]. Here we reconstruct bottom water [CO_3^{2-}] variability from B/Ca ratios of benthic foraminifera and indicators of sedimentary dissolution, and use these reconstructions to infer the flow of northern-sourced deep water to the deep central sub-Antarctic Atlantic Ocean. We find that nearly every Dansgaard–Oeschger interstadial is accompanied by a rapid incursion of North Atlantic Deep Water into the deep South Atlantic. Based on these results and transient climate model simulations[7], we conclude that North Atlantic stadial–interstadial climate variability was associated with significant Atlantic overturning circulation changes that were rapidly transmitted across the Atlantic. However, by demonstrating the persistent role of Atlantic overturning circulation changes in past abrupt climate variability, our reconstructions of carbonate chemistry further indicate that the carbon cycle response to abrupt climate change was not a simple function of North Atlantic overturning.

The presence of Dansgaard–Oeschger (D–O) variability in glacial climate archives[1] extending from Greenland ice cores[2,8] to North Atlantic sediment cores[9], tropical hydroclimate records[10] and Antarctic ice cores[4] bears witness to a global organizing element of abrupt climate change. These millennial-scale climate anomalies exhibit a distinct north–south dipole expression, as documented by the tight yet 'asynchronous' coupling of Antarctic climate variability with Northern Hemisphere climate across D–O cycles[4]. The widely accepted explanation of the observed millennial-scale climate oscillations in both hemispheres is that they represent freshwater-induced perturbations of the Atlantic Meridional Overturning Circulation (AMOC) and the associated cross-equatorial meridional heat transport[5]. Despite the strong support from conceptual[11] and numerical model simulations[3,12,13], unequivocal proxy evidence in support of an oceanic role in inter-hemispheric D–O climate variability as well as potential underlying trigger mechanisms is lacking. A key question that remains unresolved in the observational record is whether significant AMOC changes contributed to all D–O cycles, exclusively to those that coincided with Heinrich events, or only a subset of these.

We investigate the character of AMOC changes during D–O versus Heinrich stadials (HS) by reconstructing changes in the export of North Atlantic Deep Water (NADW) to the central sub-Antarctic Atlantic from variations in bottom water [CO_3^{2-}] in sediment core MD07-3076Q (Fig. 1; 44° 09.2′ S, 14° 13.7′ W, 3,770 m water depth). Our proxy data provide a Southern Hemisphere perspective on two key aspects of D–O climate variations: their association with large-scale dynamical adjustments of the Atlantic overturning, and the impact of these on deep Atlantic carbonate chemistry and carbon cycling (Fig. 1).

Sediment core MD07-3076Q has been accurately dated by 59 radiocarbon measurements on monospecific planktonic foraminifer samples[14] and has been stratigraphically aligned to rate changes in Antarctic temperature by means of abundance variations of the planktonic cold-water foraminifer *Neogloboquadrina pachyderma* sinistral (s.)[15] (see Supplementary Information for more details). Sedimentation rates during the last glacial period are 15 cm kyr^{-1} on average, which minimizes any significant impact of bioturbation on our proxy reconstructions.

The study site is presently bathed in Lower Circumpolar Deep Water in the transition zone between low-[CO_3^{2-}] southern-sourced Antarctic Bottom Water (AABW), and high-[CO_3^{2-}] northern-sourced NADW (Fig. 1). The proximity of the core site to carbonate (that is, calcite) saturation ($\Omega = [CO_3^{2-}]_{in\text{-}situ}/[CO_3^{2-}]_{saturated} = 1.09$; Supplementary Information) makes it highly sensitive to lateral shifts of the NADW/AABW boundary and associated changes in Ω (Fig. 1). It has been shown that the gradient between [CO_3^{2-}] of the glacial equivalents of NADW and AABW increased during the last glacial[16], hence increasing the sensitivity of our core site to changes in the presence of northern- versus southern-sourced water masses during the last glacial period.

We infer changes in bottom water [CO_3^{2-}] using B/Ca ratios of the epibenthic foraminifer *Cibicides kullenbergi*[17] and auxiliary sedimentary partial dissolution proxies. The dissolution and chemical destruction of foraminifera, when exposed to corrosive, low-[CO_3^{2-}] bottom- and/or pore water, more strongly affects the thin-walled and fragile shells of planktonic foraminifera than the robust shells of benthic foraminifera[18]. We therefore also derive variations in carbonate saturation at the core site from changes

[1]Godwin Laboratory for Palaeoclimate Research, Earth Sciences Department, University of Cambridge, Downing Street, Cambridge CB2 3EQ, UK. [2]LSCE/IPSL, Laboratoire CNRS-CEA-UVSQ, 91198 Gif-sur-Yvette, France. [3]Climate Change Research Centre, University of New South Wales, Sydney, New South Wales 2052, Australia. [4]ARC Centre of Excellence for Climate System Science, Sydney, New South Wales 2052, Australia. [5]International Pacific Research Center, Department of Oceanography, SOEST, University of Hawaii, 96822 Honolulu, USA. *e-mail: jg619@cam.ac.uk

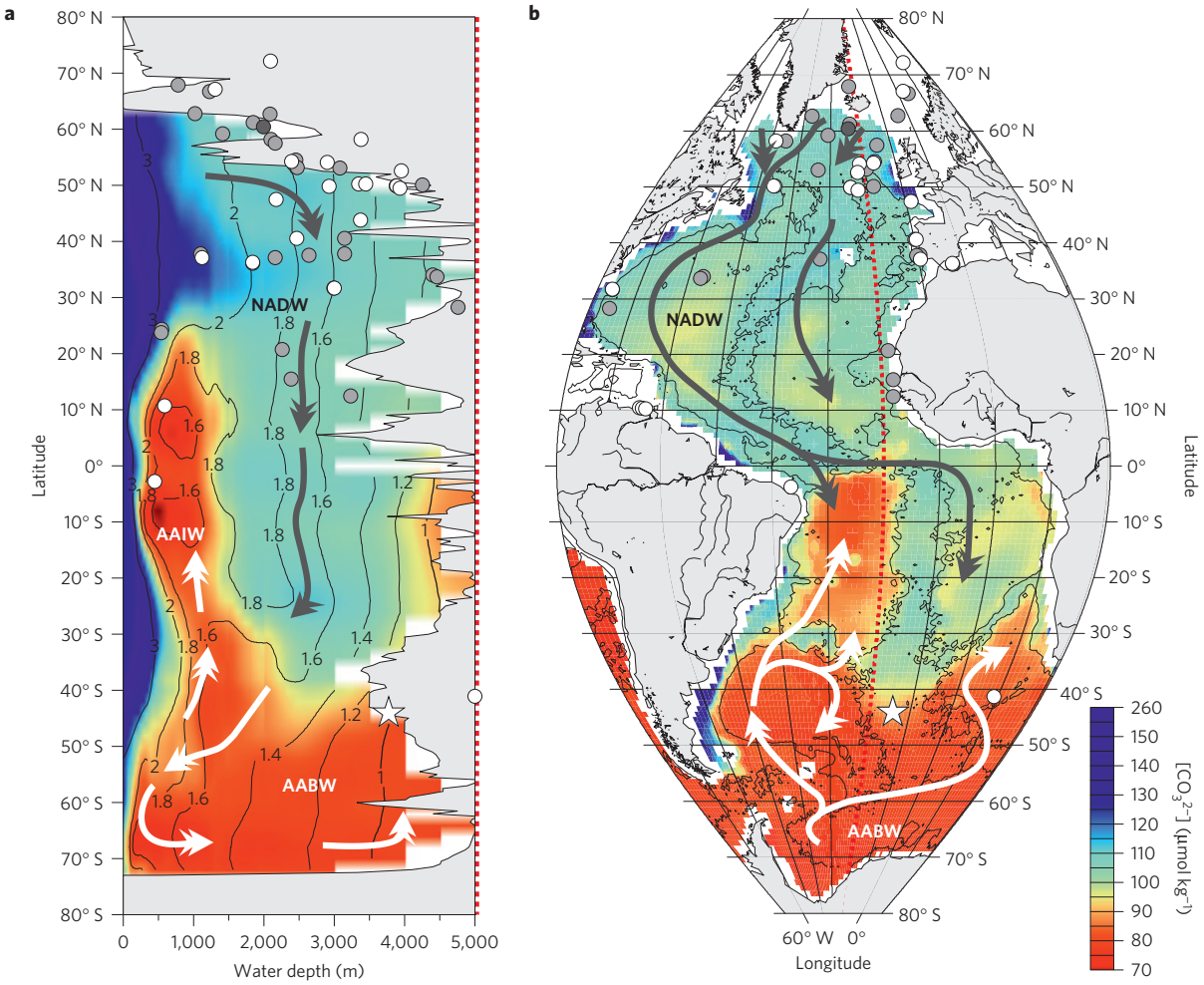

Figure 1 | Atlantic Ocean [CO_3^{2-}]. a, Meridional [CO_3^{2-}] transect along 20° W showing the calcite saturation $\Omega = [CO_3^{2-}]_{in\text{-}situ}/[CO_3^{2-}]_{saturated}$ (contoured) and **b**, areal section of the bottom water [CO_3^{2-}], where the thin black line tracks the 4,000 m-isobath (see Supplementary Information for details). Grey and white arrows show the flow path of northern-sourced (NADW, North Atlantic Deep Water) and southern-sourced (AAIW, Antarctic Intermediate Water; AABW, Antarctic Bottom Water) water masses, respectively. Circles show sediment cores documenting millennial-scale climate variations in the surface ocean (white), the surface and deep ocean (grey), and the deep ocean only (dark grey; Supplementary Table 1). The stars mark the location of the study core.

in the degree of foraminifer shell fragmentation, the ratio of benthic to planktonic (Be/Pl) foraminifera and the abundance of planktonic foraminifera in MD07-3076Q sediments (Fig. 2). To remove potential biases of the individual proxies and to increase the signal-to-noise ratio of reconstructed carbonate saturation changes, we construct a composite sub-Antarctic 'saturation index' by normalizing and subsequently averaging all sedimentary dissolution indicators (Fig. 2 and Supplementary Information).

Carbonate saturation and sedimentary partial dissolution proxies consistently indicate rapid millennial-scale changes of the bottom water corrosiveness at the core site that show a remarkable co-variation with climate fluctuations recorded in the North Atlantic and over Greenland (Fig. 2a–f). Carbonate preservation was enhanced during D–O interstadials, whereas strong dissolution events coincided with D–O and Heinrich stadials during the past 70 kyr (Fig. 2a–f). Epibenthic B/Ca-based [CO_3^{2-}] varied by ~30 μmol kg^{-1}, ranging from absolute values commonly observed in the modern deep Southern Ocean during stadials (~80 μmol kg^{-1}) to values observed in the modern deep North Atlantic during interstadials (~110 μmol kg^{-1}; Fig. 2c). Reconstructed [CO_3^{2-}] fell slightly below levels that are observed in the modern deep Southern Ocean between 33 and 20 kyr before present (BP), which includes the Last Glacial Maximum (LGM) period (Fig. 2c). Although absolute age model uncertainties of ~1,600 ± 500 years[15] (Supplementary Information) preclude an unequivocal validation, the observed close resemblance of deep sub-Antarctic carbonate saturation changes and Northern Hemisphere D–O climate signals (Fig. 2) as well as the high temporal correlation between them (up to $R^2 = 0.5$, statistically significant above the 95% level; Supplementary Information) suggest a tight coupling of North Atlantic D–O climate variability and deep sub-Antarctic Atlantic [CO_3^{2-}] throughout the last glacial period.

The strongest millennial-scale carbonate undersaturation events during the last glacial period coincide with HS4, HS5, HS5a and HS6, consistent with observations in the Cape Basin[19] (Fig. 2h–j), and suggest the incursion of very corrosive 'pure' southern-sourced waters and the rapid retreat of high-[CO_3^{2-}] NADW from the core site[19–21]. Although long-term interglacial–glacial changes in the ocean carbonate system might have driven deep, sub-Antarctic Atlantic [CO_3^{2-}] to their minimum levels during the LGM (ref. 22), it seems clear that millennial-scale carbonate saturation changes during the last glacial period were instead primarily linked with abrupt lateral shifts of (geochemical) water mass boundaries in the deep sub-Antarctic Atlantic during North Atlantic Heinrich stadials.

However, whereas previous studies failed to identify a significant response in Southern Ocean deep water properties/tracers during

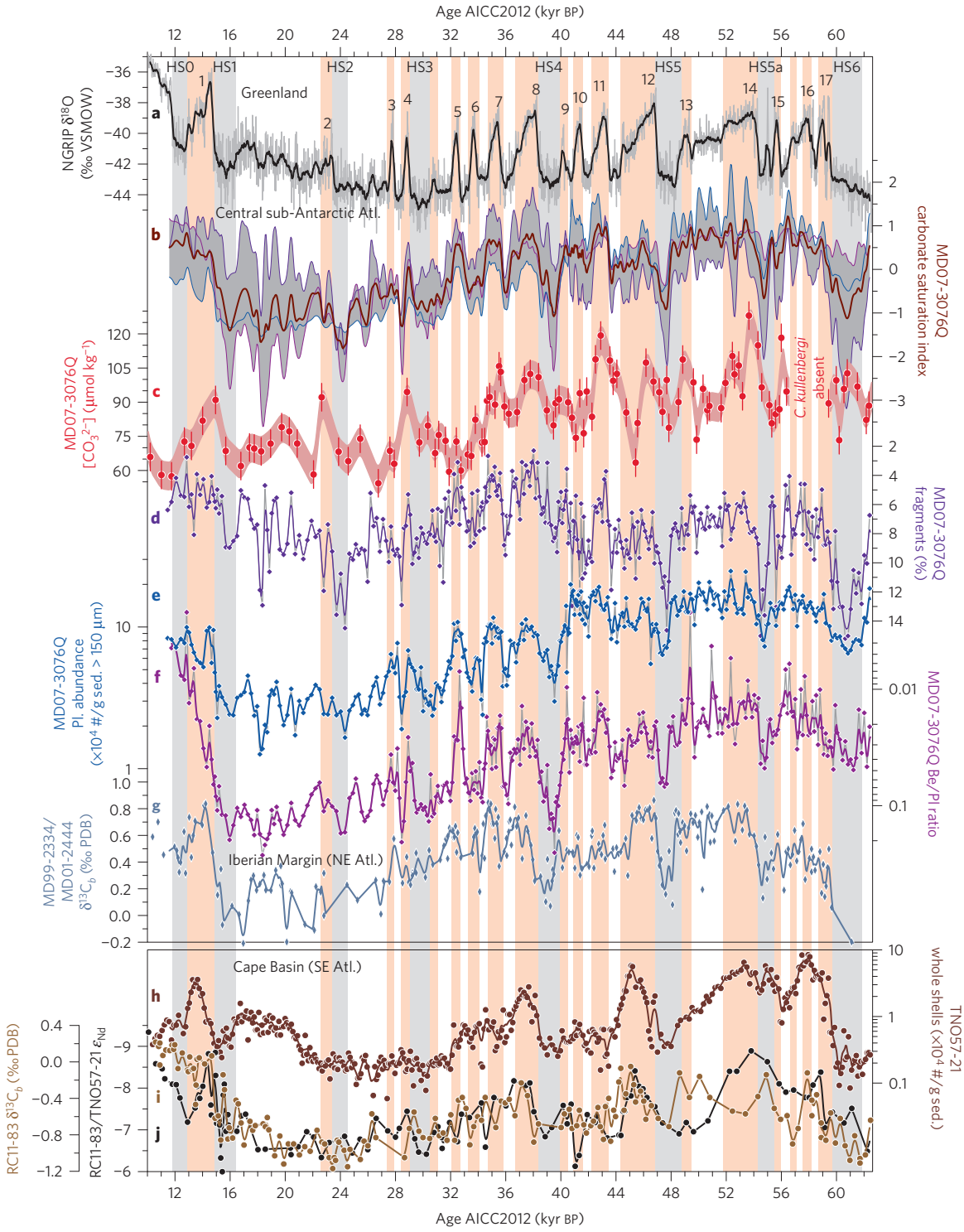

Figure 2 | High-resolution Greenland and Atlantic climate records. a, NGRIP ice core $\delta^{18}O$ (ref. 8). **b**, Carbonate 'saturation index' inferred from planktonic foraminifer shell fragmentation (purple, **d**), planktonic foraminifer abundances (blue, **e**) and the benthic:planktonic foraminifer ratio (magenta, **f**) in MD07-3076Q. **c**, *C. kullenbergi* B/Ca-based [CO_3^{2-}] estimates (envelope: 2σ-uncertainties). **g**, Epibenthic $\delta^{13}C$ in Iberian Margin cores MD99-2334 and MD01-2444 (ref. 9). **h**, Foraminifer shell abundances in Cape Basin core TNO57-21 (ref. 19). **i**, Epibenthic $\delta^{13}C$ in Cape Basin core RC11-83 (ref. 20). **j**, Water mass source indicator ε_{Nd} in RC11-83 and TNO57-21 (ref. 21). Lines, 300-year running averages. Bars, Dansgaard–Oeschger events (D–O; orange)[2], Heinrich stadials (HS; grey)[23].

D–O cycles or during minor Heinrich stadials[19–21] that are generally associated with a weaker freshwater forcing in the North Atlantic[23], such as HS2 and HS3 (Fig. 2h–j), we find clear evidence for enhanced carbonate dissolution in the deep sub-Antarctic during all Heinrich stadials, including HS2 and HS3, as well as during nearly all non-Heinrich D–O stadials (Fig. 2a–f). The suppressed expression of D–O 6, D–O 13 and D–O 16 may be explained by chronostratigraphic uncertainties and/or a decreased sensitivity of carbonate dissolution to particularly short events (Supplementary Information). The findings suggest that all North Atlantic stadials

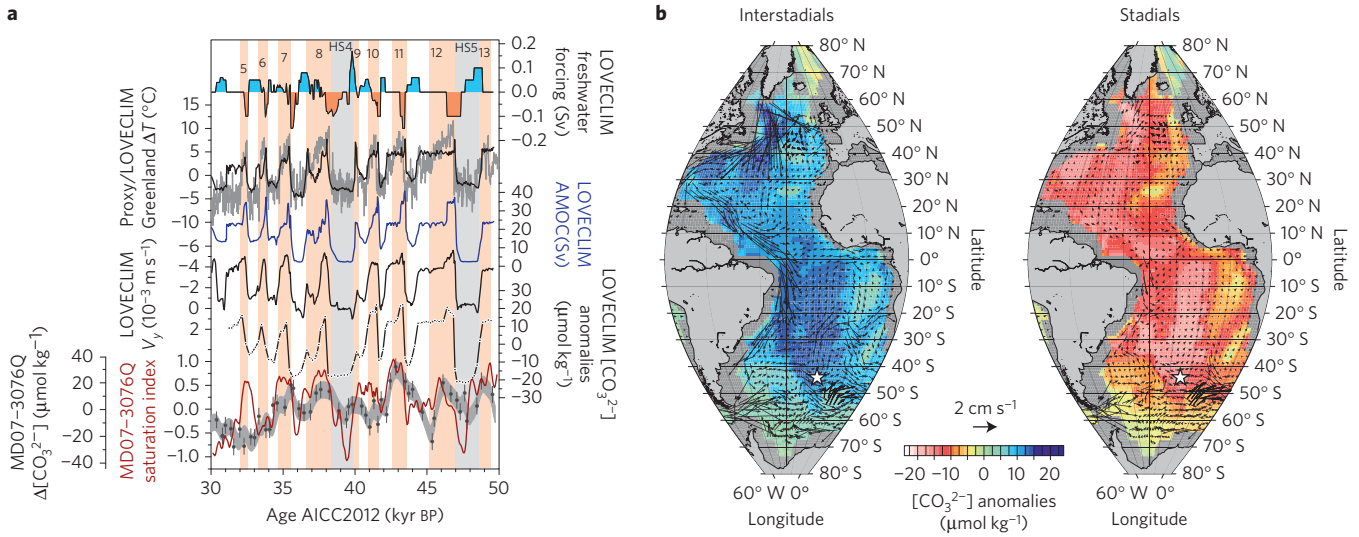

Figure 3 | Model–proxy data comparison. a, Top to bottom: North Atlantic freshwater forcing in LOVELCIM (ref. 7), proxy-based (grey) and simulated (black) Greenland air temperature anomalies (ΔT; ref. 7), simulated maximum Atlantic Meridional Overturning (AMOC) streamfunction[7], simulated meridional current velocities (negative: southward) at the study site, modelled [CO_3^{2-}] anomalies at the study site, reconstructed $\Delta[CO_3^{2-}]$ (grey; $\Delta[CO_3^{2-}] = [CO_3^{2-}]_{in\text{-}situ} - [CO_3^{2-}]_{saturated}$; envelope: 2σ-uncertainties) and carbonate saturation variations (red) in MD07-3076Q. Bars and annotations as in Fig. 2. **b**, Simulated mean interstadial (left) and stadial (right) bottom water [CO_3^{2-}] anomalies (shaded) and current velocities (vectors) in the deep Atlantic (>2 km) (see Supplementary Information for details on the calculation). The stars mark the location of MD07-3076Q.

were associated with a reduction in the contribution of NADW in the sub-Antarctic Atlantic, consistent with similarly paced, albeit less clearly expressed, changes in deep water properties in the North Atlantic[9] (Fig. 2g). Although our proxy data cannot fully unravel the exact underlying mechanisms, for example, changes in the formation rate of NADW and/or AABW, Atlantic–Pacific exchange and/or [CO_3^{2-}] endmember changes, they support previous interpretations[4] by providing evidence for rapid and recurring changes in deep water mass structure in the sub-Antarctic Atlantic, and therefore for perturbations of the AMOC in parallel with Northern Hemisphere D–O cycles.

To gain a better understanding of the South Atlantic's carbonate ion response to Northern Hemisphere D–O variability, we analyse the Atlantic [CO_3^{2-}] variations simulated by the Earth system model LOVECLIM, which includes estimates of the freshwater, orbital, greenhouse and ice-sheet forcing history for the period 50-30 kyr BP (ref. 7; Supplementary Information). The simulation is in close agreement with marine and terrestrial palaeoclimate records from both hemispheres[7]. Periods of strong (weak) freshwater forcing over the North Atlantic correspond to a weaker (stronger) simulated AMOC and a respective change in meridional heat transport, cold (warm) North Atlantic conditions, and lower (higher) values of [CO_3^{2-}] at the sub-Antarctic core site, which is in excellent agreement with the proxy data (Fig. 3 and Supplementary Information). Simulated stadial–interstadial [CO_3^{2-}] anomalies of ~30 μmol kg^{-1} at the core location correspond to changes in the model's AMOC index within 170 ± 20 years (Fig. 3a and Supplementary Information). The abrupt and closely coupled response of the simulated AMOC and [CO_3^{2-}] changes, as well as of the reconstructed carbonate saturation index and Northern Hemisphere D–O cycles, suggests an unexpectedly rapid 'transmission' of D–O surface climate signals into the deep sub-Antarctic Atlantic within a few centuries (Supplementary Information).

The rapid transmission of D–O climate anomalies in the model (and arguably in the proxy data) may be explained by two simultaneously operating mechanisms[24,25]: North Atlantic climate anomalies are linked with surface ocean density anomalies that are propagated through the global ocean via sub-surface ocean (that is, Kelvin- and Rossby) waves[24]. This causes a fast whole-ocean adjustment of pressure gradients (that is, three-dimensional shifts of density surfaces) within decades to centuries[24], and triggers anomalous meridional currents in the South Atlantic (Fig. 3 and Supplementary Information) that act on the steep mean South Atlantic meridional [CO_3^{2-}] gradient. For stadial–interstadial transitions, for instance, this generates a southward shift of the sub-Antarctic [CO_3^{2-}] front due to the southward transport of high-[CO_3^{2-}] water masses in the sub-Antarctic Atlantic. In addition, perturbations in the formation and/or the pathway of NADW generate an advective and diffusive adjustment of water mass properties in the Atlantic[25] that, along with amplifying effects from other processes such as variations in the accumulation of respired organic carbon, strongly contribute to the total adjustment of [CO_3^{2-}] at the sub-Antarctic Atlantic core site (Fig. 3 and Supplementary Information). Through these processes (rapid buoyancy-induced wave propagation and tracer advection anomalies) geochemical properties in the deep South Atlantic remain tightly coupled to AMOC anomalies originating in the North Atlantic (within 170 ± 20 years).

Other mechanisms that might explain the rapid connection from the North Atlantic to the Southern Ocean include atmospheric connections[26] and subsequent changes to the mean position and strength of Ekman divergence. However, simulated Southern Hemisphere westerly wind stress varies by only 10% during AMOC changes and may therefore play only a minor role for deep sub-Antarctic Atlantic [CO_3^{2-}] anomalies compared to the changes brought about by perturbations of the AMOC (Supplementary Information). Overall, the Earth system model simulation supports the notion of an ocean-mediated and fast adjustment of the carbonate saturation state in the deep sub-Antarctic Atlantic in response to D–O-related North Atlantic density anomalies.

Although these findings directly document the previously inferred[4] close coupling of AMOC perturbations and D–O climate anomalies, they also carry implications for carbon cycle feedbacks associated with abrupt climate changes. Antarctic ice-core records demonstrate that atmospheric CO_2 increased most clearly during Heinrich stadials[27]. If the reconstructed reductions in sub-Antarctic [CO_3^{2-}] during these stadial periods affected a sufficiently large ocean volume and reflected a more efficient 'organic carbon pump'[28], they would imply an increase in the total dissolved inorganic carbon

inventory of the deep Atlantic and Southern Ocean. In this case, the observed atmospheric CO_2 rise during stadials would have to result from either: increased ventilation of the Pacific[29], enhanced carbon release from terrestrial sources[30], and/or a significant increase in the extent of equilibration between the low-[CO_3^{2-}] deep Southern Ocean and the atmosphere[14]. The absence of significant changes in atmospheric CO_2 during short North Atlantic stadials[27] may ultimately derive from a careful balance of some or all of these processes. Regardless of the exact mechanisms at play, which remain to be determined, the results presented here indicate that any differences in the carbon cycle response during D–O and Heinrich stadials[27] cannot easily be attributed to a lack of an AMOC response during these abrupt climate events.

Methods

Methods and any associated references are available in the online version of the paper.

Received 14 February 2015; accepted 8 September 2015; published online 12 October 2015

References

1. Völker, A. H. J. *et al.* Global distribution of centennial-scale records for Marine Isotope Stage (MIS) 3: A database. *Quat. Sci. Rev.* **21,** 1185–1212 (2002).
2. Dansgaard, W. *et al.* Evidence for general instability of past climate from a 250-kyr ice-core record. *Nature* **364,** 218–220 (1993).
3. Ganopolski, A. & Rahmstorf, S. Rapid changes of glacial climate simulated in a coupled climate model. *Nature* **409,** 153–158 (2001).
4. EPICA Community Members. One-to-one coupling of glacial climate variability in Greenland and Antarctica. *Nature* **444,** 195–198 (2006).
5. Broecker, W. S., Bond, G., Klas, M., Bonani, G. & Wolfli, W. A salt oscillator in the glacial Atlantic? 1. The concept. *Paleoceanography* **5,** 469–477 (1990).
6. Lynch-Stieglitz, J. *et al.* Muted change in Atlantic overturning circulation over some glacial-aged Heinrich events. *Nature Geosci.* **7,** 144–150 (2014).
7. Menviel, L., Timmermann, A., Friedrich, T. & England, M. H. Hindcasting the continuum of Dansgaard–Oeschger variability: Mechanisms, patterns and timing. *Clim. Past* **10,** 63–77 (2014).
8. North Greenland Ice Core Project Members. High-resolution record of Northern Hemisphere climate extending into the last interglacial period. *Nature* **431,** 147–151 (2004).
9. Skinner, L. C., Elderfield, H. & Hall, M. in *Ocean Circulation: Mechanisms and Impacts* (eds Schmittner, A., Chiang, J. C. H. & Hemming, S. R.) 197–208 (Geophysical Monograph Series, American Geophysical Union, 2007).
10. Deplazes, G. *et al.* Links between tropical rainfall and North Atlantic climate during the last glacial period. *Nature Geosci.* **6,** 213–217 (2013).
11. Stocker, T. F. & Johnsen, S. J. A minimum thermodynamic model for the bipolar seesaw. *Paleoceanography* **18,** 1087 (2003).
12. Schmittner, A., Saenko, O. A. & Weaver, A. J. Coupling of the hemispheres in observations and simulations of glacial climate change. *Quat. Sci. Rev.* **22,** 659–671 (2003).
13. Timmermann, A., Gildor, H., Schulz, M. & Tziperman, E. Coherent resonant millennial-scale climate oscillations triggered by massive meltwater pulses. *J. Clim.* **16,** 2569–2585 (2003).
14. Skinner, L. C., Fallon, S., Waelbroeck, C., Michel, E. & Barker, S. Ventilation of the deep Southern Ocean and deglacial CO_2 rise. *Science* **328,** 1147–1151 (2010).
15. Gottschalk, J., Skinner, L. C. & Waelbroeck, C. Contribution of seasonal sub-Antarctic surface water variability to millennial-scale changes in atmospheric CO_2 over the last deglaciation and Marine Isotope Stage 3. *Earth Planet. Sci. Lett.* **411,** 87–99 (2015).
16. Yu, J., Elderfield, H. & Piotrowski, A. M. Seawater carbonate ion- $\delta^{13}C$ systematics and application to glacial–interglacial North Atlantic ocean circulation. *Earth Planet. Sci. Lett.* **271,** 209–220 (2008).
17. Yu, J. & Elderfield, H. Benthic foraminiferal B/Ca ratios reflect deep water carbonate saturation state. *Earth Planet. Sci. Lett.* **258,** 73–86 (2007).
18. Berger, W. H. Planktonic foraminifera: Selective solution and paleoclimatic interpretation. *Deep-Sea Res. I* **15,** 31–43 (1968).
19. Barker, S. & Diz, P. Timing of the descent into the last ice age determined by the bipolar seesaw. *Paleoceanography* **29,** 489–507 (2014).
20. Charles, C. D., Lynch-Stieglitz, J., Ninnemann, U. S. & Fairbanks, R. G. Climate connections between the hemisphere revealed by deep sea sediment core/ice core correlations. *Earth Planet. Sci. Lett.* **142,** 19–27 (1996).
21. Piotrowski, A. M., Goldstein, S. L., Hemming, S. R. & Fairbanks, R. G. Temporal relationships of carbon cycling and ocean circulation at glacial boundaries. *Science* **307,** 1933–1938 (2005).
22. Hodell, D. A., Charles, C. D. & Sierro, F. J. Late Pleistocene evolution of the ocean's carbonate system. *Earth Planet. Sci. Lett.* **192,** 109–124 (2001).
23. Hemming, S. R. Heinrich events: Massive late Pleistocene detritus layers of the North Atlantic and their global climate imprint. *Rev. Geophys.* **42,** RG1005 (2004).
24. Timmermann, A., Krebs, U., Justino, F., Goosse, H. & Ivanochko, T. Mechanisms for millennial-scale global synchronization during the last glacial period. *Paleoceanography* **20,** PA4008 (2005).
25. Goodman, P. J. Thermohaline adjustment and advection in an OGCM. *J. Phys. Oceanogr.* **31,** 1477–1497 (2001).
26. Dong, B.-W. & Sutton, R. T. Adjustment of the coupled ocean–atmosphere system to a sudden change in the Thermohaline Circulation. *Geophys. Res. Lett.* **29,** http://dx.doi.org/10.1029/2002GL015229 (2002).
27. Ahn, J. & Brook, E. J. Siple Dome ice reveals two modes of millennial CO_2 change during the last ice age. *Nature Commun.* **5,** 3723 (2014).
28. Schmittner, A., Brook, E. J. & Ahn, J. in *Ocean Circulation: Mechanisms and Impacts* Vol. 173 (eds Schmittner, A., Chiang, J. C. H. & Hemming, S. R.) 209–246 (Geophysical Monograph Series, American Geophysical Union, 2007).
29. Menviel, L., England, M. H., Meissner, K. J., Mouchet, A. & Yu, J. Atlantic-Pacific seesaw and its role in outgassing CO_2 during Heinrich events. *Paleoceanography* **29,** 58–70 (2014).
30. Köhler, P., Joos, F., Gerber, S. & Knutti, R. Simulated changes in vegetation distribution, land carbon storage, and atmospheric CO_2 in response to a collapse of the North Atlantic thermohaline circulation. *Clim. Dynam.* **25,** 689–708 (2005).

Acknowledgements

We are indebted to D. Hodell for his insightful comments. J.G. was funded by the Gates Cambridge Trust. L.C.S. would like to acknowledge NERC grant NE/J010545/1 and the Royal Society. S.M. was supported by ERC grant 2010-NEWLOG ADG-267931 HE. C.W. acknowledges support from the European Research Council grant ACCLIMATE/no 339108. L.M. was supported by the Australian Research Council grant DE150100107. A.T. acknowledges support from the US NSF (grants 1400914, 1341311). Model experiments were performed on a computational cluster owned by the Faculty of Science of the University of New South Wales, Australia. This is LSCE contribution 5353 and IPRC publication number 1131.

Author contributions

J.G. and L.C.S. designed the study. C.W. collected the core material. J.G. performed census counts and measured the epibenthic trace element composition under the guidance of S.M. at the University of Cambridge. J.G. and L.C.S. analysed the proxy data. L.M. and A.T. contributed model output data and the interpretation thereof. J.G., L.C.S. and A.T. wrote this manuscript with contributions from all authors.

Additional information

Supplementary information is available in the online version of the paper. Reprints and permissions information is available online at www.nature.com/reprints. Correspondence and requests for materials should be addressed to J.G.

Competing financial interests

The authors declare no competing financial interests.

Methods

Chronology. The chronostratigraphy of sediment core MD07-3076Q is based on 59 monospecific planktonic foraminifer radiocarbon dates that have been corrected for variable reservoir ages[14], as well as the stratigraphic alignment of down-core abundance variations of the cold-water species *N. pachyderma* (s.) with changes in Antarctic temperature[15] reflected by the first derivative of the δD record of the Antarctic EPICA Dome C (EDC) ice core on the AICC2012 age scale (see Supplementary Information for a detailed description). The *N. pachyderma* (s.) abundance- and the radiocarbon-derived age models deviate from each other by only 500 $\pm$ 400 years—therefore agreeing within age model uncertainties in the overlapping core section[15]. Uncertainties of the radiocarbon-based age–depth markers increase strongly before 27 kyr BP owing to a lack of reservoir age constraints[14] and increasing uncertainties of the atmospheric calibration curves[31]. Age–depth markers that result from the radiocarbon- and *N. pachyderma* (s.) abundance-based chronostratigraphic models have therefore been spliced at 27 kyr BP, applying the calibrated radiocarbon age constraints for the core section younger than 27 kyr BP and the *N. pachyderma* (s.) abundance-based chronology for the core section older than 27 kyr BP (ref. 15; Supplementary Figs 1 and 2). The final chronology is based on a linear interpolation between the tie points[15]. Chronological uncertainties amount to about 1,200 $\pm$ 400 years for the period between 27 and 10 kyr BP (ref. 14) and to 1,600 $\pm$ 500 years before 27 kyr BP (ref. 15).

The reported age model of sediment core MD07-3076Q (refs 14,15) is consistent with an alignment of abundance variations of the planktonic foraminifer *Globigerina bulloides* with EDC δD (Supplementary Fig. 1). Abundance variations of *G. bulloides* have been proposed to parallel Antarctic temperature variations owing to various adaptation strategies of this planktonic species to environmental and climatic changes[32]. The agreement between the two age model approaches therefore supports the applied core chronology[14,15] (Supplementary Information).

Reconstruction of bottom water carbonate ion concentrations. The variability of deep water $[CO_3^{2-}]$ is inferred from B/Ca ratios of the epibenthic foraminifer *C. kullenbergi* (>212 µm) by applying a sensitivity of 0.69 µmol mol^{-1} change in calcite B/Ca ratios per µmol kg^{-1} deviation of *in situ* $[CO_3^{2-}]$ from saturation levels ($\Delta[CO_3^{2-}]$; ref. 17). Past $[CO_3^{2-}]$ changes at the study site are calculated as the deviation of $\Delta[CO_3^{2-}]_{down-core}$ from pre-industrial saturation $[CO_3^{2-}]$ at the core site (87.3 µmol kg^{-1}; ref. 17; for details on the calculation of the applied pre-industrial $[CO_3^{2-}]$ parameters with the CO_2SYS program[33], see Supplementary Information). Epibenthic foraminifera have been chemically cleaned following the reductive–oxidative method (Supplementary Information) and weighed 90–430 µg before cleaning, which is equivalent to 5–20 specimens per measurement. Contamination levels have been monitored on the basis of foraminiferal Mn/Ca, Fe/Ca and Al/Ca ratios, which suggest no major impact of contaminant phases on epibenthic B/Ca ratios (Supplementary Information).

Census counts. Marine sediment samples were disintegrated in deionized water, washed over a mesh to remove fine-grained clay particles and subsequently dried in an oven at temperatures <50 °C. Sedimentary dissolution parameters have been determined from census counts of a sample aliquot of the size fraction >150 µm containing at least 300 planktonic foraminifer grains. The fragmentation is reported as the percentage of fragmented grains to the number of whole planktonic foraminifera. Only those fragmented shells have been considered that comprise approximately half or more of the original shell, circumventing the application of correction factors for the degree of fragmentation of a single foraminifera[34]. The one-sigma uncertainty of determined foraminifer shell fragmentation amounts to 1.9% (n = 15). The abundance of planktonic foraminifera has been calculated from census counts taking into account the number of sample splits and is reported as the number of foraminifera per gram dry sediment (>150 µm size fraction). One-sigma uncertainties of determined planktonic abundance and the Be/Pl ratio variations in the sediment are 6,000 foraminifera per gram sediment >150 µm and 0.014, respectively (n = 15).

To construct a composite 'carbonate saturation index' of sub-Antarctic bottom waters, we normalized our smoothed (300-year running average) dissolution proxy records. The foraminiferal shell fragmentation and Be/Pl ratio records have been inverted to obtain a consistent notation. The 'saturation index' represents the average of all normalized records.

Data. Data reported in this study are stored in the PANGAEA database (http://doi.pangaea.de/10.1594/PANGAEA.841244, http://doi.pangaea.de/10.1594/PANGAEA.837069). Three-dimensional fields of the physical variables of the transient simulation of Marine Isotope Stage 3 performed with LOVECLIM (ref. 7) can be found at: http://apdrc.soest.hawaii.edu/las/v6/dataset?catitem=6290.

NGRIP δ^{18}O data[8] and EDC δD data[35] are available at http://www.iceandclimate.nbi.ku.dk/data and https://www.ncdc.noaa.gov/cdo/f?p=519:1:0::::P1_STUDY_ID:6080, respectively. The applied age scale of the ice-core records can be obtained from the supplementary data of ref. 36 (http://www.clim-past.net/9/1733/2013/cp-9-1733-2013-supplement.zip).

Data from sediment cores TNO57-21 and RC11-83 (refs 19–21,37) have recently been compiled in the supplementary data of ref. 19 (http://onlinelibrary.wiley.com/doi/10.1002/2014PA002623/full).

Epibenthic δ^{13}C data from Iberian Margin cores[9] can be downloaded from http://doi.pangaea.de/10.1594/PANGAEA.738036 and http://doi.pangaea.de/10.1594/PANGAEA.849505.

The CO_2SYS program is available from http://cdiac.ornl.gov/oceans/co2rprt.html.

Code availability. We have opted not to make the computer codes associated with this paper available because they are based on simple FERRET data analysis and visualization as well as MATLAB commands.

References

31. Reimer, P. J. *et al.* IntCal13 and Marine13 radiocarbon age calibration curves 0–50,000 years cal BP. *Radiocarbon* **55,** 1869–1887 (2013).
32. Barker, S. *et al.* Interhemispheric Atlantic seesaw response during the last deglaciation. *Nature* **457,** 1097–1102 (2009).
33. Lewis, E. & Wallace, D. W. R. *Program developed for CO_2 system calculations* (Carbon Dioxide Information Analysis Center, Oak Ridge National Laboratory, US Dept. of Energy, 1998).
34. Le, J. & Shackleton, N. J. Carbonate dissolution fluctuations in the western equatorial Pacific during the late Quaternary. *Paleoceanography* **7,** 21–42 (1992).
35. Jouzel, J. *et al.* Orbital and millennial Antarctic climate variability over the past 800,000 years. *Science* **317,** 793–796 (2007).
36. Veres, D. *et al.* The Antarctic ice core chronology (AICC2012): An optimized multi-parameter and multi-site dating approach for the last 120 thousand years. *Clim. Past* **9,** 1733–1748 (2013).
37. Ninnemann, U. S., Charles, C. D. & Hodell, D. A. in *Mechanisms of Global Climate Change at Millennial Time Scales* Vol. 112 (eds Clark, P. U., Webb, R. S. & Keigwin, L. D.) 99–112 (American Geophysical Union, 1999).